Pressure-Induced Invar Behavior in Pd_3Fe

M. L. Winterrose,[1] M. S. Lucas,[1] A. F. Yue,[1] I. Halevy,[1] L. Mauger,[1] J. A. Muñoz,[1] Jingzhu Hu,[2] M. Lerche,[3] and B. Fultz[1]

[1]*California Institute of Technology, W. M. Keck Laboratory 138-78, Pasadena, California 91125, USA*
[2]*National Synchrotron Light Source, University of Chicago, Upton, New York 11973, USA*
[3]*HPSynC, Carnegie Institution of Washington, Argonne, Illinois 60439, USA*

(Received 24 February 2008; published 10 June 2009)

Synchrotron x-ray diffraction (XRD) measurements, nuclear forward scattering (NFS) measurements, and density functional theory (DFT) calculations were performed on $L1_2$-ordered Pd_3Fe. Measurements were performed at 300 K at pressures up to 33 GPa, and at 7 GPa at temperatures up to 650 K. The NFS revealed a collapse of the ^{57}Fe magnetic moment between 8.9 and 12.3 GPa at 300 K, coinciding with a transition in bulk modulus found by XRD. Heating the sample under a pressure of 7 GPa showed negligible thermal expansion from 300 to 523 K, demonstrating Invar behavior. Zero-temperature DFT calculations identified a ferromagnetic ground state and showed several antiferromagnetic states had comparable energies at pressures above 20 GPa.

DOI: 10.1103/PhysRevLett.102.237202 PACS numbers: 75.50.Bb, 62.50.−p, 71.20.Be, 76.80.+y

The Invar effect has remained a topic of interest since Guillaume discovered the low thermal expansion of Fe-Ni alloys in 1897 [1]. Today ''Invar behavior'' has come to mean a broad range of anomalies in magnetic and mechanical properties, including molar volume, elastic moduli, heat capacity, magnetization, high field susceptibility, and others [2]. Iron-rich fcc-based Invar alloys are characterized by the existence of nearly degenerate states with differing magnetic moments and volumes [3] (and refs. therein). Decreasing the Fe concentration stabilizes the magnetically ordered state, and suppresses thermal Invar behavior. Recently, it was discovered [4] that some Fe-Ni alloys with normal thermal expansion properties at ambient pressure exhibit Invar behavior at high pressure.

Alloys of Fe-Pd with compositions around 30% Pd have long been known for Invar behavior at ambient pressure [5]. In addition to Invar behavior, Fe-Pd exhibits several other anomalies in mechanical and magnetic behavior such as a martensitic transformation in Fe-rich samples [6], giant magnetic moment formation [7], noncollinear magnetic states [8], and anisotropy in the spin-wave dispersions in Pd-rich alloys [9]. Here, we report pressure-induced Invar behavior in Pd-rich Pd_3Fe with the ordered $L1_2$ structure. At ambient pressure, Pd_3Fe is ferromagnetically ordered with a Curie temperature (T_c) measured between 500 K [10] and 540 K [11], and magnetic moments at room temperature of $2.73 \pm 0.13\mu_B$ and $0.51 \pm 0.05\mu_B$ at the Fe and Pd sites, respectively [12]. We report that the ferromagnetic ground state is destabilized with pressure, and a magnetic collapse begins around 10 GPa, accompanied by an increase in bulk modulus at pressures after the magnetic collapse. We also find that at a pressure near the start of the magnetic collapse, ordered Pd_3Fe exhibits a near-zero thermal expansion from 300 to 523 K.

Samples of $Pd_3^{57}Fe$ were prepared by arc-melting Pd of 99.95% purity and ^{57}Fe of 95.38% isotopic enrichment. There was no measurable mass loss or visible surface oxidation after melting the 100 mg ingots. The material was cold rolled to a thickness of 25 μm. The $L1_2$ chemical long-range order was obtained by annealing at 700 °C for 16 hours, followed by annealing at 600 °C for 24 hours, and a subsequent cooling to 20 °C over 2 hours. X-ray diffraction confirmed the $L1_2$ structure with a rolling texture consistent with $(011)[2\bar{1}\bar{1}]$.

Room temperature x-ray diffraction (XRD) measurements were performed at pressures up to 33 GPa at beam line X17C of the National Synchrotron Light Source (NSLS) at Brookhaven National Laboratory (BNL). Energy-dispersive x-ray diffraction (EDXD) data were acquired with a polychromatic x-ray beam and a Ge detector at a fixed Bragg angle of 12°. A Merrill-Bassett diamond-anvil cell [13] with 500 μm culets and a 250 μm chamber was used with silicone oil as the pressure medium, with pressure calibration by the fluorescence of ruby technique [14]. No crystallographic phase transition was observed under pressure.

Figure 1 shows volume vs pressure data for ordered Pd_3Fe from the EDXD measurements. A significant volume collapse was found between approximately 10 and 15 GPa, and a reduced slope in the volume-pressure data was found above 15 GPa. The EDXD data were fit successfully to the ''Weiss-like equation of state'' of [15] which models the low-pressure and high-pressure regions with two separate Murnaghan [16] equations of state. The region around the volume collapse is modeled as a weighed sum of the high-pressure and low-pressure equations of state, with a thermodynamic occupancy factor based on the assumption that the energies of the electronic energy levels have a linear dependence on pressure. The fit to the low-pressure region up to 10 GPa gave a zero-pressure bulk modulus (B_0) of 229 ± 2 GPa and a ground state lattice parameter (a_0) of 3.849 ± 0.002 Å, the latter result in good agreement with previous studies [17]. The high-pressure region from 16.5 to 33 GPa gave a B_0 of 286 ± 3 GPa and

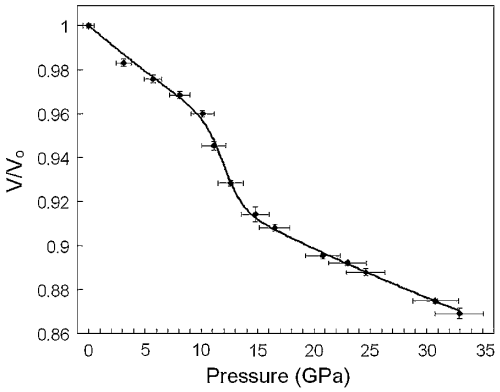

FIG. 1. Volume-pressure data obtained from synchrotron x-ray diffraction measurements (symbols) and the fit of the data to the Weiss-like equation of state [15] (line).

an a_0 of 3.792 ± 0.005 Å. The pressure derivative of the bulk modulus was fixed to the typical metallic value of 4.0 in all cases. In the volume-collapse region from 10 to 16.5 GPa, fitting to the ''Weiss-like equation of state'' gave a transition pressure between the low-pressure and high-pressure regions of 12.1 ± 0.1 GPa and a pressure range for the transition of 0.9 ± 0.1 GPa.

Nuclear forward scattering (NFS) spectrometry offers a direct measure of the magnetic state under pressure, and was performed at 300 K at beam line 16ID-D at the Advanced Photon Source (APS) at the Argonne National Laboratory (ANL) using the same diamond anvil cell [13]. Figure 2 shows NFS spectra from ordered $Pd_3^{57}Fe$ at pressures up to 25.3 GPa. The transition region of Fig. 2 follows well the transition region shown in Fig. 1. Quantum beats, expected from a magnetically ordered material, are prominent in the NFS spectra at lower pressures. The quantum beats decrease significantly in amplitude at 12.3 GPa, and vanish at the highest pressures. They do not change significantly in their time modulation, however. This is consistent with a first-order phase transition, where pressure replaces a high magnetization state with a low magnetization state.

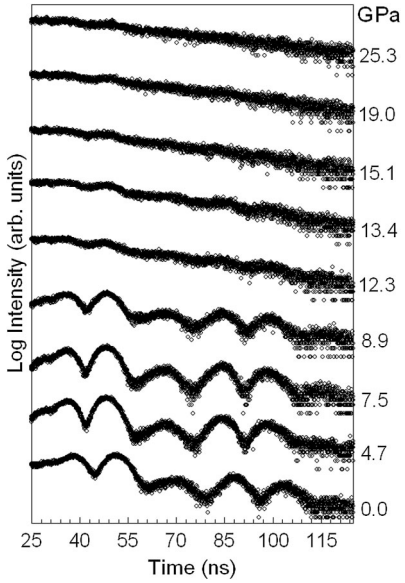

FIG. 2. Nuclear forward scattering spectra from ordered $Pd_3^{57}Fe$ showing an abrupt decrease of the hyperfine magnetic fields in the material around 12 GPa.

In another EDXD experiment, the $Pd_3^{57}Fe$ sample was heated under pressure in a diamond anvil cell with a resistive heating furnace (D'Anvils Ltd.) at beam line X17C of the NSLS. Au powder was used as an internal pressure calibrator inside the cell during the heating. Measurements were taken at a pressure of 7 GPa (± 0.1 GPa at the lower temperatures), heating to a maximum temperature of 673 K. Figure 3 shows the results of these measurements. The Au expands at all temperatures while the Pd_3Fe shows practically no thermal expansion up to 523 K. (Above 600 K, there was a more rapid loss of pressure in the cell. We expect this would reverse some of the Invar transition leading to an artificially large thermal expansion at the highest temperatures of Fig. 3.)

We performed floating moment density functional theory (DFT) calculations in the local spin-density approximation (LSDA) [18] for the electronic exchange and correlation potential using the Vienna *ab initio* simulation package (VASP) [19]. The interaction between the electrons and ions used the projector augmented-wave (PAW) method [20], treating the semicore $2p$ states in Fe and $3p$ states in Pd as valence. Calculations were performed for a ferromagnetic state (FM), a state of ferrimagnetic order (FR), in which the spin on the central Fe atom in a 32 atom supercell is reversed with respect to the other spins, a low-spin state (LS), and three antiferromagnetic states, which we denote AFM-I, AFM-II, and AFM-III. In the LS state studied, the moments at the Fe and Pd sites couple ferromagetically with their combined magnetic moment in the unit cell never exceeding $0.01\mu_B$. In the AFM-I state, Fe moments order in alternating ferromagnetic sheets in the (110) plane. The AFM-II state has Fe moments order-

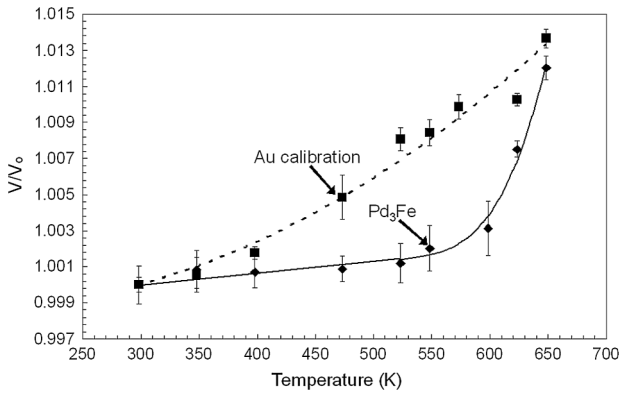

FIG. 3. Volume-temperature data for $Pd_3^{57}Fe$ (diamonds) and Au (squares) obtained from externally heating the diamond anvil cell at an approximately constant pressure of 7 GPa. The $Pd_3^{57}Fe$ shows practically no thermal expansion up to 523 K. The solid and dashed lines are guides for the eye.

ing ferromagnetically in alternating (100) planes, while in the AFM-III state, they order ferromagnetically in alternating (111) planes. Different energy cutoffs for the plane wave basis sets and different k-space grids were used for the various magnetic structures owing to the different supercells. In all cases, total energies were converged with respect to both k-points and energy cutoff to better than 1 meV/atom. For each magnetic state, energy versus volume data were obtained by first relaxing the geometry according to the conjugate-gradient algorithm, then performing a series of single-point energy calculations about the equilibrium volume. The resulting energy-volume data were fitted to the Murnaghan equation of state [16], giving parameters listed in Table I.

This procedure gave a FM ground state with a lattice parameter of 3.802 Å at 0 GPa and 0 K with magnetic moments of 3.16 and $0.33\mu_B$ within spheres of radius 1.486 Å around the Fe and Pd sites (similar to earlier spin-polarized DFT results [21,22]). The calculated lattice parameter is slightly smaller than the experimental result, as is expected for the LSDA, while the magnetic moments are in good agreement with saturation moments [23]. Over a large volume range from 9 to 15 Å^3/atom, the FM, AFM-I, AFM-II, and FR states are all extremely close in energy, never separated by more than 9 meV/atom, and have similar elastic properties. The AFM-III structure is within 37 meV/atom in this same volume range. With increasing pressure, the FM state is destabilized, leading to a transition to the AFM-I state at $a = 3.690$ Å. The magnetic moments in the AFM-I state decrease gradually with decreasing volume, disappearing completely by $a = 3.148$ Å (see Fig. 4). If only the FM and LS states are taken into account, a transition to the LS state takes place at $a = 3.355$ Å, where the FM moment on the Fe site drops discontinuously from $1.39\mu_B$ to $0.008\mu_B$. Such behavior would be qualitatively similar to that predicted for disordered $Fe_{70}Pt_{30}$ [24], with a larger stability range for the AFM state in Pd_3Fe.

The LS state is stable only at very high pressures, but its elastic properties show similarities to the high-pressure state in the experimental studies. There is a significantly higher B_0 and lower V_0 in the LS state, similar to those of the transition found in the EDXD data and the NFS data of Figs. 1 and 2, but the calculated transitions occur at very different pressures. The EDXD measurements show a volume collapse beginning around 10.1 GPa, or $V/V_0 = 0.96$, ending by 14.8 GPa, or $V/V_0 = 0.91$, similar to that of the FM to AFM-I transition found in our DFT calculations ($V/V_0 = 0.91$). The DFT calculations do not give a stable LS state until a much higher compression ($V/V_0 = 0.57$). In the LSDA, some discrepancy between theoretical and experimental transition pressures is expected, and a higher pressure is typical, but this discrepancy is larger than expected.

TABLE I. Parameters obtained from DFT calculations of energy versus volume, fitted to the Murnaghan equation of state.

	Fit Range(Å^3/atom)	B_0 (GPa)	B_0'	a_0 (Å)
FM	$12.33 \leq V \leq 15.07$	216.81	5.12	3.802
AFM-I	$12.21 \leq V \leq 14.92$	216.39	5.03	3.798
AFM-II	$12.48 \leq V \leq 14.66$	217.79	5.02	3.800
AFM-III	$12.54 \leq V \leq 15.00$	218.19	5.15	3.800
FR	$12.27 \leq V \leq 15.00$	218.06	5.06	3.801
LS	$11.84 \leq V \leq 14.48$	242.59	5.11	3.760

We discuss two possible interpretations. The simplest is that the LSDA is greatly underestimating the relative stability of the LS magnetic state, and a high-spin (HS) to LS transition occurs around $V/V_0 = 0.96$ instead of the calculated $V/V_0 = 0.57$. This view is supported by the similarities in the changes in B_0 and V_0 between the HS and LS states in the calculations and experiments. Further support is given by the excellent fit to the EDXD data with the Weiss-like equation of state, which is based on the assumption of the Weiss 2-γ model [25] of a transition between a HS state at low pressures to a LS state at high pressures.

An alternative explanation is possible. There will also be a collapse of the ^{57}Fe hyperfine magnetic field if the moments fluctuate at a rate of 10^9 Hz or higher. At ambient pressure, the magnetic ordering temperature in Pd_3Fe is ~500 K. Pressure is known to have a strong effect on the value of T_c in Invar alloys [2,26] (and refs. therein). Increasing the pressure above 10 GPa may reduce T_c to below room temperature in Pd_3Fe, where a spin disordering transition can occur. Nevertheless, the Fe moments in Pd_3Fe are well localized [22], and the Fe atoms likely retain most of their moments in the paramagnetic state. This paramagnetic state is to be distinguished from a truly nonmagnetic state in which no local moments exist in the material [27]. The magnitude of the discrepancy between the experimental and theoretical transition pressures leads us to favor this alternative explanation. Nevertheless, a significant change in the local magnetic moment magni-

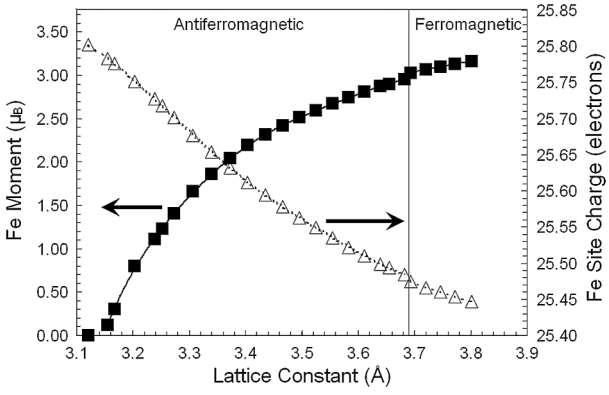

FIG. 4. Magnetic moments at the Fe site (left), and charge at the Fe site (right) versus the lattice constant of Pd_3Fe from DFT calculations. Antiferromagnetic refers to the AFM-I structure (see text). The solid and dashed lines are guides to the eye.

tude could accompany this transition, as discussed for Fe-Pt and Fe-Pd [28].

A quantitative account of the spontaneous volume magnetostriction in Invar has been given for Fe-Pt and Fe-Pd [28] using the disordered local moment method (DLM) [29]. These studies identified the necessary condition for Invar behavior as having an alloy at the edge of the transition from strong to weak ferromagnetism; i.e., the Fermi level (E_F) must be at the top of the majority $3d$ band in the ferromagnetic state. Thermal excitations cause a relatively large decrease in the local Fe moments, and large magnetovolume effects around the transition temperature. Our calculations show that alloying with Pd causes the top of the majority $3d$ band to move to energies below E_F, stabilizing the strong ferromagnetic state and suppressing the Invar effect, in agreement with [28]. On the other hand, our calculations show that applying external pressure gives the opposite trend, as the antibonding states at the top of the majority $3d$ band move up in energy towards E_F. Pressure therefore counteracts the band-filling effect of Pd, bringing an anomalously large spontaneous volume magnetostriction to Pd_3Fe. By tuning the position of the top of the $3d$ band with respect to E_F, pressure-induced Invar behavior resembles classical Invar behavior that is controlled by chemical composition.

We thank Y. Xiao and P. Chow for assistance with the NFS measurements, J. McCorquodale and M. Kresch for computational support, and to O. Delaire for helpful discussions. This work was supported by the Carnegie-DOE Alliance Center (CDAC), funded by the U.S. Department of Energy (DOE) through the Stewardship Sciences Academic Alliance (SSAA) of the National Nuclear Security Administration (NNSA). Use of the APS, ANL, was supported by DOE, Office of Science, Office of Basic Energy Sciences (BES), under Contract No. DE-AC02-06CH11357. HPCAT (Sector 16) was supported by DOE-BES, DOE-NNSA, the National Science Foundation (NSF), and the W. M. Keck Foundation. Use of the NSLS, BNL, was supported by DOE-BES, under Contract No. DE-AC02-98CH10886. Beam line X17C at NSLS was supported by the Consortium for Materials Properties Research in Earth Sciences (COMPRES) of NSF.

[1] C. E. Guillaume, C.R. Hebd. Seances Acad. Sci. **125**, 235 (1897).
[2] E. F. Wassermann, in *Ferromagnetic Materials*, edited by K. H. J. Buschow and E. P. Wohlfarth (North- Holland, Amsterdam, 1990), Vol. 5, p. 237.
[3] D. D. Johnson *et al.*, in *Physical Metallurgy of Controlled Expansion Invar-Type Alloys*, edited by K. C. Russel and D. F. Smith (TMS, Warrendale, PA 1990), p. 3; I. A. Abrikosov *et al.*, Phys. Rev. B **76**, 014434 (2007).
[4] L. Dubrovinsky *et al.*, Phys. Rev. Lett. **86**, 4851 (2001).
[5] A. Kussmann and K. Jessen, J. Phys. Soc. Japan Suppl. **17B1**, 136 (1962).
[6] T. Sohmura *et al.*, Scr. Metall. **14**, 855 (1980); R. Oshima, Scr. Metall. **19**, 315 (1985).
[7] J. Crangle and W. R. Scott, J. Appl. Phys. **36**, 921 (1965); G. G. Low, Adv. Phys. **18**, 371 (1969).
[8] Y. Tsunoda and R. Abe, Phys. Rev. B **55**, 11507 (1997); Y. Tsunoda and R. Abe, Physica B (Amsterdam) **237–238**, 458 (1997); R. Abe *et al.*, J. Phys. Condens. Matter **10**, L79 (1998).
[9] A. J. Smith *et al.*, J. Phys. F **7**, 2411 (1977).
[10] G. Longworth, Phys. Rev. **172**, 572 (1968).
[11] M. Fallot, Ann. Phys. (Paris) **10**, 291 (1938).
[12] S. J. Pickart and R. Nathans, J. Appl. Phys. **33**, 1336 (1962); V. A. Tsurin and A. Z. Men'shikov, Phys. Met. Metallogr. **45**, 82 (1978); A. Z. Men'shikov and V. A. Tsurin, Phys. Met. Metallogr. **47**, 68 (1979).
[13] E. Sterer *et al.*, Rev. Sci. Instrum. **61**, 1117 (1990).
[14] A. Jayaraman, Rev. Mod. Phys. **55**, 65 (1983).
[15] L. Nataf *et al.*, Phys. Rev. B **74**, 184422 (2006).
[16] F. D. Murnaghan, Proc. Natl. Acad. Sci. U.S.A. **30**, 244 (1944).
[17] M. Hansen, *Constitution of Binary Alloys, Metallurgy and Metallurgical Engineering Series* (McGraw-Hill, New York, 1958), 2nd ed.
[18] D. M. Ceperley and B. J. Alder, Phys. Rev. Lett. **45**, 566 (1980); J. P. Perdew and A. Zunger, Phys. Rev. B **23**, 5048 (1981).
[19] G. Kresse and J. Furthmüller, Comput. Mater. Sci. **6**, 15 (1996); Phys. Rev. B **54**, 11169 (1996).
[20] P. E. Blöchl, Phys. Rev. B **50**, 17953 (1994); G. Kresse and D. Joubert, Phys. Rev. B **59**, 1758 (1999).
[21] C. A. Kuhnen *et al.*, Phys. Rev. B **35**, 370 (1987); C. A. Kuhnen *et al.*, Phys. Rev. B **46**, 8915 (1992); S. K. Bose *et al.*, J. Magn. Magn. Mater. **87**, 97 (1990); T. Nautiyal *et al.*, Phys. Scr. **46**, 527 (1992); Y. S. Shi *et al.*, Phys. Rev. B **65**, 172410 (2002).
[22] P. Mohn *et al.*, Aust. J. Phys. **46**, 651 (1993).
[23] J. W. Cable *et al.*, Phys. Rev. **138**, A755 (1965).
[24] Sergii Khmelevskyi and Peter Mohn, Phys. Rev. B **68**, 214412 (2003).
[25] R. J. Weiss, Proc. Phys. Soc. London **82**, 281 (1963); J. Kaspar and D. R. Salahub, Phys. Rev. Lett. **47**, 54 (1981); P. Entel *et al.*, Phys. Rev. B **47**, 8706 (1993); E. Duman *et al.*, Phys. Rev. Lett. **94**, 075502 (2005); M. Matsushita *et al.*, Phys. Rev. B **77**, 064429 (2008).
[26] P. Gorria *et al.*, Phys. Status Solidi (RRL) **3**, 115 (2009).
[27] P. Mohn, *Magnetism in the Solid State, Springer Series in Solid State Sciences* (Springer-Verlag, Berlin, Heidelberg, 2003), Vol. 134.
[28] S. Khmelevskyi *et al.*, Phys. Rev. Lett. **91**, 037201 (2003); S. Khmelevskyi and P. Mohn, Phys. Rev. B **69**, 140404 (2004); S. Khmelevskyi *et al.*, Phys. Rev. B **72**, 064510 (2005).
[29] B. L. Gyorffy *et al.*, J. Phys. F **15**, 1337 (1985); F. J. Pinski *et al.*, Phys. Rev. Lett. **56**, 2096 (1986).